



Pulsed ultrasound-modulated optical tomography using spectral-hole burning as a narrowband spectral filter

Youzhi Li, Huiliang Zhang, Chulhong Kim, Kelvin H. Wagner, Philip Hemmer, and Lihong V. Wang

Citation: [Applied Physics Letters](#) **93**, 011111 (2008); doi: 10.1063/1.2952489

View online: <http://dx.doi.org/10.1063/1.2952489>

View Table of Contents: <http://scitation.aip.org/content/aip/journal/apl/93/1?ver=pdfcov>

Published by the [AIP Publishing](#)

Articles you may be interested in

[Lock-in camera based heterodyne holography for ultrasound-modulated optical tomography inside dynamic scattering media](#)

Appl. Phys. Lett. **108**, 231106 (2016); 10.1063/1.4953630

[Spectral-domain optical coherence tomography: Removal of autocorrelation using an optical switch](#)

Appl. Phys. Lett. **88**, 111115 (2006); 10.1063/1.2186520

[Ultrasound-modulated optical speckle measurement for scattering medium in a coaxial transmission system](#)

Appl. Phys. Lett. **87**, 063504 (2005); 10.1063/1.2009058

[Broadband InGaAs tapered diode laser sources for optical coherence radar and coherence tomography](#)

Appl. Phys. Lett. **86**, 191101 (2005); 10.1063/1.1925313

[Ultrasound-modulated optical computed tomography of biological tissues](#)

Appl. Phys. Lett. **84**, 1597 (2004); 10.1063/1.1651330

The image shows the cover of the journal Applied Physics Reviews. It features a blue and orange color scheme with a molecular structure in the background. The text 'AIP Applied Physics Reviews' is at the top left. The main title 'NEW Special Topic Sections' is in large white letters. Below it, 'NOW ONLINE' is in yellow, followed by 'Lithium Niobate Properties and Applications: Reviews of Emerging Trends' in white. The AIP logo and 'Applied Physics Reviews' are at the bottom right.

NEW Special Topic Sections

NOW ONLINE
Lithium Niobate Properties and Applications:
Reviews of Emerging Trends

AIP Applied Physics
Reviews

Pulsed ultrasound-modulated optical tomography using spectral-hole burning as a narrowband spectral filter

Youzhi Li,¹ Huiliang Zhang,² Chulhong Kim,¹ Kelvin H. Wagner,³ Philip Hemmer,² and Lihong V. Wang^{1,a)}

¹Biomedical Engineering Department, Washington University in St Louis, St. Louis, Missouri 63130, USA

²Electrical and Computer Engineering Department, Texas A&M University, College Station, Texas 77843, USA

³Electrical and Computer Engineering Department, University of Colorado at Boulder, Boulder, Colorado 80309, USA

(Received 21 February 2008; accepted 2 June 2008; published online 11 July 2008)

We applied a submegahertz nonlinear optical filter afforded by a cryogenically cooled spectral-hole burning crystal to ultrasound-modulated optical tomography. Our experimental results show that this technique, having the largest *etendue* among all available ultrasound-modulated optical tomography techniques and being immune to speckle decorrelation, offers potential for imaging *in vivo* and forming high resolution optical tomograms in real time. It opens an opportunity for the development of a clinically applicable high resolution optical imaging modality. © 2008 American Institute of Physics. [DOI: 10.1063/1.2952489]

Ultrasound-modulated optical tomography^{1–3} (UOT) attracts increasing interest for biomedical applications because it is capable of simultaneously achieving good resolution and imaging depth. This technique fuses the mature ultrasound (US) technique and the promising optical imaging by employing the acousto-optic interaction effect. In UOT, a near-infrared coherent laser illuminates a thick tissue perturbed by a focused US wave. A portion of the multiply scattered photons propagating through the US field is modulated due to the US-induced scatterer's displacements and local refractive index change,⁴ yielding modulation sidebands. The photons at the sidebands carry spatial information about the soft tissue and are used to form an optical image, while the unmodulated dc light contributes as a noise source. The lateral resolution of the optical image is determined by the focused US beam width, and the axial resolution is achieved by using either frequency-swept US waves⁵ or US pulses.⁶

The detection of the US-modulated photons in UOT is, however, a demanding task. The modulated photons are usually weak (this is particularly true when high frequency short US pulses are used to obtain submillimeter resolution) and spatially incoherent (time-varying speckles). Several detection schemes have been proposed. A single fast detector^{2,3} was used to detect the modulation of the speckle pattern at the applied US frequency. The optical *etendue* ($G=S\Omega$, where S is the detector active area, and Ω is the acceptance solid angle) is limited because only one or a few speckles can be detected, and the detected modulation depth otherwise decreases by $1/\sqrt{N}$,³ where N is the number of the speckles. A confocal Fabry-Pérot interferometer⁷ (CFPI) has been employed to filter one sideband of the UOT signals while suppressing the dc and the other modulation sideband. This technique also suffers from a small *etendue*. Multipixel charge-coupled device (CCD) detection scheme⁸ can process multiple speckles in parallel, providing a better *etendue*. However, it may not be applicable to *in vivo* imaging scenarios due to the slow CCD frame rates and the fast decorrelation rate of the speckles. The photorefractive effect af-

forded by a bismuth silicon oxide crystal has recently been adopted to interferometrically detect the US-modulated photons.⁹ This technique has a larger *etendue* over the aforementioned approaches. However, its applicability is still limited by the response time, $\tau_{PR} \approx 100$ ms, of the crystal since speckle patterns generated by *in vivo* biological tissues usually have a decorrelation time less than 1 ms. A faster response time can be obtained by employing GaAs crystals¹⁰ along with a strong reference beam. Yet, the deployment of these fast GaAs crystals in UOT is challenging since one has to simultaneously fight against a low light coupling efficiency as well as a strong, scattered reference light, which is a dominant noise source in these systems. The lack of an efficient detection mechanism has so far prevented the promising UOT from being developed into a reliable and clinically applicable imaging tool.

Here, we present a technique for efficient detection of US-modulated photons by using a narrowband absorptive filter achieved with spectral-hole burning (SHB). This technique is capable of selecting one sideband of the UOT signal while suppressing the strong dc speckles and the other sideband. This system offers UOT the potential for a large *etendue* as well as the capability of spectrally filtering in parallel many speckles with submegahertz spectral resolution. Since our system is based on transmitting the US-modulated optical speckles through a frequency-dependent absorptive filter constructed from an SHB crystal, it is inherently immune to speckle decorrelation, potentially allowing *in vivo* imaging.

SHB has been extensively investigated for various applications.^{11–13} An SHB medium¹⁴ is a rare-earth ion doped, inhomogeneously broadened optical absorber, which can be modeled as a two-level system.¹⁵ When cryogenically cooled, it has a submegahertz homogeneous linewidth $\Delta\Gamma_H$ and an inhomogeneous bandwidth $\Delta\Gamma_I$ of gigahertz. Each homogeneous frequency can be individually accessed using a proper narrow laser line excitation. When a monochromatic laser source at frequency f_L illuminates a cryogenically cooled SHB crystal, the resonant ions are excited from their ground states to the excited states, resulting in an absorption coefficient $\alpha(f)$ change at f_L . Sufficiently intense illumina-

a) Author to whom correspondence should be addressed. Electronic mail: lhwang@biomed.wustl.edu.

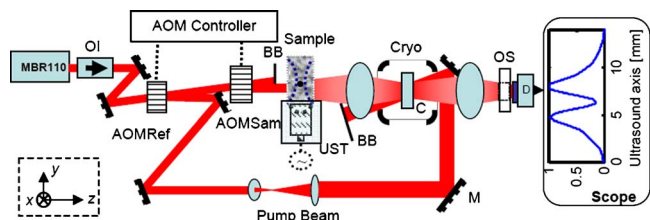


FIG. 1. (Color online) Experimental setup. OI: optical isolator. AOM: acousto-optic modulator. UST: US transducer. Cryo: cryostat. C: crystal. BB: beam block. M: mirror. OS: optical shutter. D: detector. Bottom-left inset: laboratory coordinates: US axis: y , light axis: z , and sample scanning axis: x .

tion excites nearly all of the resonant ions, and as a consequence, a spectral transparency is engraved at f_L with line-width of $\Delta\Gamma_H$ in the spectral absorption band of the crystal. For an optically dense SHB crystal [$\alpha(f)L_c \gg 1$, where L_c is the crystal thickness], a deep spectral hole engraved at f_L significantly reduces the absorption coefficient $\alpha(f_L)$, yet $\alpha(f \neq f_L)$ stays unchanged, leaving the crystal in a highly absorptive state across $\Delta\Gamma_L$ other than at f_L . This feature is ideal for use in detecting the US-modulated photons in UOT. The transmitted US-modulated, spatially speckled light has the strong dc light suppressed by the SHB crystal so that the information-carried speckles can simply be incoherently integrated to yield UOT signals with a high signal-to-noise ratio.

The present SHB UOT system is schematically shown in Fig. 1. The SHB crystal used in our proof-of-concept system is a $10 \times 9 \times 1.5$ mm³ 2% at Tm³⁺:YAG (yttrium aluminum garnet) crystal. Its working wavelength at 793 nm is preferred for biomedical imaging, and solid state laser sources at this wavelength are readily available. The optical absorption length is measured as $\alpha(f)L=4$, yielding a dc suppression of 18 dB, governed by Beer's law $I_{dc}^{out}=I_{dc}^{in}\exp(-\alpha L)$. A cw Ti:sapphire laser (Coherent MBR110), pumped by a frequency-doubled diode laser (Coherent Verdi 10 W), is utilized as the source and operates at 793.38 nm with an output of 2 W. The laser beam is first frequency shifted by 70 MHz with an IntraAction acousto-optic modulator (AOM) labeled as AOMRef in Fig. 1 (AOM802A1) driven by one channel of an IntraAction dual channel frequency synthesizer (DFE-754A4-16), generating 980 mW, 3.3 ms long optical pulses. These pulses are used as the pump beam, which is beam expanded to cover the 9 mm diameter clear aperture of the crystal. The crystal is cryogenically cooled to ~ 4 K with a cryostat (Janis, Model: STVP-400). The pump beam burns transparent spectral holes across the crystal's clear aperture [$\alpha(70 \text{ MHz})L=0.9$, and $\alpha(f \neq 70 \text{ MHz})L=4$, corresponding to a 14 dB transmission improvement at this frequency] forming a number of narrowband bandpass filters, which have a lifetime of about 10 ms. After the narrowband bandpass filters are engraved, the AOMRef is turned off and another AOM of the same model, AOMSam, is turned on with a driven frequency at 75 MHz, equal to the AOMRef driven frequency plus the US frequency of 5 MHz. Light pulse, which is 20 μ s in duration and 500 mW in peak power, diffracted off the AOMSam is beam-shaped to a 0.3×8 mm² elliptical beam to illuminate the $50 \times 50 \times 10$ mm³ issue-mimicking phantom sample. The sample consists of 10% porcine skin gelatine (Sigma G2500) and 1% Intralipid, yielding a reduced scattering coefficient of $\mu'_s \approx 7 \text{ cm}^{-1}$ at the wavelength of 793 nm. A two-cycle 5 MHz US pulse

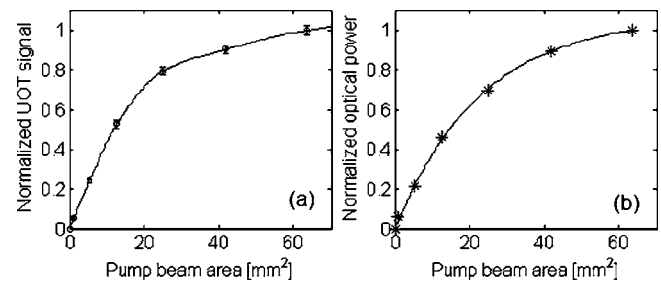


FIG. 2. Parallel speckle processing. (a) UOT signal (circles) as a function of the pump beam size, and the shape preserved fitting (solid line). Error bars: the propagated standard deviations. (b) Total optical power (stars) vs the pump beam size, and the theoretical fitting (solid line) for the Gaussian distributed pump beam.

with a peak pressure of 4.3 MPa is simultaneously launched into the sample through water using a focusing transducer (Panametrics-NDT, Model: A326S-SU, focal length: 16.2 mm, focal spot size: 0.5 mm). The US pulse has a mechanical index (defined as the ratio of the US peak pressure in megapascal to the square root of its central frequency in megahertz) of 1.9, which is within the US safety limit.¹⁶ The US pulse forms a volumetric ultrasonic field of 0.12 mm³ (speed of sound in tissue = 1.5 mm/ μ s) in the transducer's focal zone, determining the spatial resolution of the final tomograms. The multiply scattered light distributed along the US propagation direction is sequentially modulated by this US volume as the US pulse propagates through the sample, allowing the creation of a spatial map of the optical properties of the sample along the US path (the so-called A-line), as shown in Fig. 1 scope trace, where the dip indicates the position of an absorber buried inside the sample. The acousto-optic interaction yields two primary weak sidebands at 70 and 80 MHz in addition to a strong unmodulated dc speckle field. The US-modulated diffused light is passed through the SHB crystal, where the 70 MHz spectral filters with a bandwidth of 720 kHz (full width at half maximum) have been engraved. The spectral filters transmit the sideband of 70 MHz while significantly attenuating the strong unmodulated dc and the other sideband at 80 MHz. The transmitted speckles are detected using a large area Si detector (Thorlabs, PDA55). The output of the detector is amplified by 50 times with a low-noise amplifier (Stanford Research, SR 560). An optical shutter (Uniblitz, VS14S2S1) is employed to time gate the pump beam from the detector to avoid detector saturation due to the scattered pump beam.

To demonstrate the capability of processing a large number of speckles in parallel, the pump beam size is varied using an iris, while the US-modulated speckles cover the entire aperture of the crystal. Figure 2(a) depicts the signal strength as a function of the pump beam size. It can be seen from the figure that the signal strength initially increases nearly linearly as the pump beam size is enlarged, and then the signal growth slows down as the pump beam size is further increased. This is mainly due to two reasons. (1) The pump beam obeys a Gaussian distribution as verified in Fig. 2(b), which burns shallower holes at its edge, yielding weaker signals. (2) The US-modulated light may not be fully diffused since the sample is thin. Otherwise, we may expect that the curve obeys a linear relationship over a larger area.

Figure 3 shows two of our imaging results. A small patterned optical absorber (Black India Ink) was buried in the middle of the tissue phantom, as shown in Fig. 3(a). The

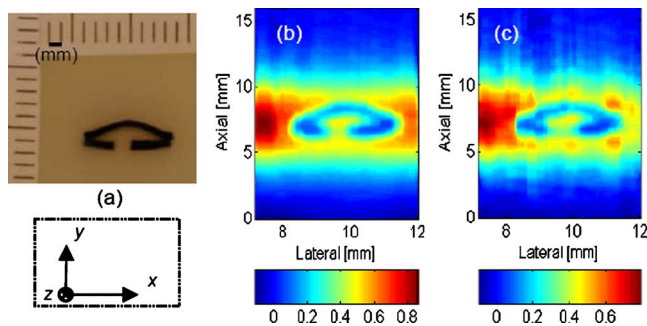


FIG. 3. (Color online) B-mode tomograms. (a). Photograph of the optical absorber buried inside the tissue phantom. (b). Tomogram with 16 times averaging. (c) Tomogram with four times averaging. Tomograms are interpolated and median filtered. Bottom-left inset: lab coordinates.

dimensions of the absorber were 0.6 mm along the US propagation direction y and 0.9 mm along the light propagation direction z . The gap at the bottom of the absorber was about 1.1 mm. It can be seen from Fig. 3(b) that the absorber has been imaged with high fidelity with only 16 times averaging for each A-line, which can potentially be completed within 320 μ s, provided that the spectral filters are engraved and 16 US pulses are fired with a repetition rate of 50 kHz. The repetition rate is so chosen that crosstalk between adjacent pulses is avoided. This speed may enable real time imaging. For this imaging speed, the optical power for each A-line imaging location is 6.7 mJ cm^{-2} , which is well below the ANSI laser safety limit at 793 nm.¹⁷

To explore the imaging speed limit of our technique, we reduced the averaging times. As shown in Fig. 3(c), a fair image can be obtained with only four times averaging, offering a potential for an 80 μ s acquisition time per A-line. We found that the major noise source that limits our current system from performing single-shot imaging is an intensity noise induced by the laser's stabilization system, whose spectrum with a spectral peak at $\sim 85 \text{ kHz}$ coincidentally overlaps with that of our UOT signals, causing artifacts on our single-shot images. However, it should be pointed out that the imaging speed as well as the overall performance of our system can be significantly improved if an optically thicker crystal is used to further suppress the strong dc and/or a balanced detector¹⁸ is employed to reject the laser noise.

The large optical *etendue* is one of the major advantages of our system. In principle, the acceptance angle of our absorption-based quantum filters can be nearly 2π , yielding an *etendue* of 1131 sr mm^2 for a $10 \times 9 \text{ mm}$ crystal aperture. In our current system, the effective *etendue* for this front-end filter is calculated as 31 sr mm^2 , limited by the numerical aperture (NA) of our cryostat windows. Yet this *etendue* is already an order of magnitude improvement over the photo-

refractive crystal based technique,¹⁹ and more than two orders of magnitude improvement over the CFPI.⁷ Moreover, the *etendue* of our system may be further improved by increasing the NA of the cryostat.

In conclusion, an original optical quantum filter implemented using a SHB crystal has been employed for detecting US-modulated photons in UOT. It processes multiple speckles in parallel and has a huge *etendue*. Since our technique is purely based on frequency-dependent absorption, it is inherently immune to speckle decorrelation, potentially allowing *in vivo* imaging. In addition, the speed of our technique offers the potential for real-time imaging. In our proof-of-feasibility experiments, we imaged tissue-mimicking phantoms with 10 mm thickness. It should be mentioned immediately that this is not the limit of our technique since the imaging depth may be improved without sacrificing the imaging speed by utilizing an optically thicker SHB crystal to further suppress the strong dc and a balanced detection scheme to reject laser intensity noise. This technique may open an opportunity to develop a reliable optical imaging system with a scalable US resolution for various biomedical applications such as early breast cancer detection.

This research was supported by the US National Institutes of Health Grant No. R33 CA 094267.

- ¹F. A. Marks, H. W. Tomlinson, and G. W. Brooksby, *Proc. SPIE* **1888**, 500 (1993); W. Leutz and G. Maret, *Physica B* **204**, 14 (1995).
- ²L. V. Wang, S. L. Jacques, and X. Zhao, *Opt. Lett.* **20**, 629 (1995).
- ³M. Kempe, M. Larionov, D. Zaslavsky, and A. Z. Genack, *J. Opt. Soc. Am. A* **14**, 1151 (1997).
- ⁴L. V. Wang, *Phys. Rev. Lett.* **87**, 043903 (2001).
- ⁵L. V. Wang and G. Ku, *Opt. Lett.* **23**, 975 (1998).
- ⁶A. Lev and B. G. Sfez, *Opt. Lett.* **28**, 1549 (2003).
- ⁷S. Sakadžić and L. V. Wang, *Opt. Lett.* **29**, 2770 (2004).
- ⁸S. Lévêque, A. C. Boccara, M. Lebec, and H. Saint-Jalmes, *Opt. Lett.* **24**, 181 (1999).
- ⁹T. W. Murray, L. Sui, G. Maguluri, R. A. Roy, A. Nieva, F. Blonigen, and C. A. DiMarzio, *Opt. Lett.* **29**, 2509 (2004).
- ¹⁰M. Lesaffre, F. Jean, F. Ramaz, A. C. Boccara, P. Delaye, and G. Roosen, *Opt. Express* **15**, 1030 (2007).
- ¹¹T. M. Mossberg, *Opt. Lett.* **7**, 77 (1982).
- ¹²L. Ménager, I. Lorgère, J. L. Le-Gouët, D. Dolfi, and J. P. Huignard, *Opt. Lett.* **26**, 1245 (2001).
- ¹³Y. Li, A. Hoskins, F. Schlottau, K. H. Wagner, C. Embry, and W. R. Babbitt, *Appl. Opt.* **45**, 6409 (2006).
- ¹⁴Y. Sun, C. W. Thiel, R. L. Cone, R. W. Equall, and R. L. Hutcheson, *J. Lumin.* **98**, 41 (2002).
- ¹⁵L. Allen and J. H. Eberly, *Optical Resonance and Two-level Atoms* (Dover, New York, 1987).
- ¹⁶D. Dalecki, *Annu. Rev. Biomed. Eng.* **6**, 229 (2004).
- ¹⁷American National Standard for the Safe Use of Lasers, Standard Z136.1-2000 (ANSI, Inc., New York, 2000).
- ¹⁸P. C. D. Hobbs, *Appl. Opt.* **36**, 903 (1997).
- ¹⁹X. Xu, H. Zhang, P. Hemmer, D. K. Qing, C. Kim, and L. V. Wang, *Opt. Lett.* **32**, 656 (2007).